
Counterfactual Maximum Likelihood Estimation for Training Deep Networks

Xinyi Wang

Department of Computer Science
UC Santa Barbara
xinyi_wang@ucsb.edu

Wenhu Chen

Department of Computer Science
UC Santa Barbara
wenhuchen@ucsb.edu

Michael Saxon

Department of Computer Science
UC Santa Barbara
saxon@ucsb.edu

William Yang Wang

Department of Computer Science
UC Santa Barbara
william@cs.ucsb.edu

Abstract

Although deep learning models have driven state-of-the-art performance on a wide array of tasks, they are prone to learning spurious correlations that should not be learned as predictive clues. To mitigate this problem, we propose a causality-based training framework to reduce the spurious correlations caused by observable confounders. We give theoretical analysis on the underlying general Structural Causal Model (SCM) and propose to perform Maximum Likelihood Estimation (MLE) on the interventional distribution instead of the observational distribution, namely Counterfactual Maximum Likelihood Estimation (CMLE). As the interventional distribution, in general, is hidden from the observational data, we then derive two different upper bounds of the expected negative log-likelihood and propose two general algorithms, Implicit CMLE and Explicit CMLE, for causal predictions of deep learning models using observational data. We conduct experiments on two real-world tasks: Natural Language Inference (NLI) and Image Captioning. The results show that CMLE methods outperform the regular MLE method in terms of out-of-domain generalization performance and reducing spurious correlations, while maintaining comparable performance on the regular evaluations.¹

1 Introduction

Deep neural networks have been tremendously successful across a variety of tasks and domains in recent years. However, studies have shown that deep learning models trained with traditional supervised learning framework tend to learn *spurious correlations* as predictive clues [1–4]. For example, in computer vision, deep learning models can rely on surface-level textures [1, 5] or background environment [2, 6] instead of the object of interest in images. In natural language processing (NLP), question-answering models are insensitive to the choice of question [7] and natural language inference models are surprisingly accurate at predicting the logical relationship between a pair of sentences from just one of them [3]. In image captioning, a phenomenon called *object hallucination* is observed where models tend to include nonexistent objects in a caption based on their common association with other objects that are actually present in the image [4].

Another related problem in the current associative learning framework, like maximum likelihood estimation (MLE), is that neural networks can achieve almost perfect performance on one dataset but

¹Our code is released at <https://github.com/WANGXinyiLinda/CMLE>.

dramatically fail to generalize on another because of a naturally occurring or adversarially enforced distribution shift [8–11]. One explanation is that the model learns ‘fake’ features induced by spurious correlations instead of invariant features that would hold in different domains for the same task [12]; this kind of invariance can be explained by the underlying causal mechanism of the task [13].

It is difficult to deal with these spurious correlations; identifying and disentangling all of their potential sources is impractical. Various training algorithms have been proposed to reduce the influence of spurious correlations by learning the underlying causal mechanism. One approach for discovering the underlying causal mechanism is by invariant prediction based on the invariance of causal mechanisms across different environments [13, 12, 14]. However, constructing such diverse environments is usually unrealistic. Another approach is counterfactual data augmentation [15–19], which directly modifies the part of the input that causes the target variable, but usually involves expensive human efforts in generating the counterfactual examples. We propose **Counterfactual Maximum Likelihood Estimation** (CMLE), which tries to perform MLE on an interventional distribution instead of the observational distribution. Here, **observational distribution** means the distribution that the train data is sampled from. **Interventional distribution** means the distribution with one or some of the variables intentionally intervened (set to some fixed value). More specifically, we aim to remove observable confounders and reduce spurious correlations by directly intervening on the label variable, without requiring human annotators or the curation of diverse environments.

In this paper, we focus on the setting of predicting the outcome Y of a certain action T on X , with the underlying causal model as $X \rightarrow Y \leftarrow T$ and an observed train dataset in the form of (X, Y, T) . Such a setting enables us to assume that there exist some observed confounders in X that influence both Y and T . This means there is potentially a false causal relation from X to T , indicated by a red arrow in Figure 1a. To further simplify our setting and to enable us to identify the counterfactual outcomes of Y , we adopt the standard Strong Ignorability assumption [20]. In our framework, instead of trying to identify all the confounders, we try to rule out the effect of the confounders by directly intervening T with a resulting causal graph as shown in Figure 1c. In this way, we explicitly take all the possible outcomes of Y into consideration during optimization. This can be viewed as mimicking a Randomized Controlled Trial (RCT), which is the gold standard approach for estimating the treatment effect [21]. The observational distribution $p(X, Y, T)$ of this setting is shown in Figure 1a and the interventional distribution $p(X, Y_1, Y_2, \dots, Y_m)$ is shown in Figure 1c.

Our method is inspired by individual treatment effect (ITE) prediction [22, 23], which tries to predict the expected effect $\mathbb{E}[Y_1 - Y_0 | X = x]$ (e.g. difference in blood pressure) of a treatment $T \in \{0, 1\}$ (e.g. drug/surgery) on a individual unit $X = x$ (e.g. a patient). In this case, the observed confounder in X can be explained by selection bias [23], which means the treatment T applied to an individual X is dependent on X . For example, young patients are more likely to be treated by surgery, while elder patients are more likely to be treated by drugs.

There are two broad kinds of tasks to which our proposed CMLE framework can apply: relationship prediction tasks that predicts the relation T given two inputs X and Y (e.g. natural language inference [24, 25], paraphrase identification [26, 27], natural language for visual reasoning [28], etc.), and conditional generation tasks that generate Y given precondition X and constraint T (e.g. style transfer [29, 30], controllable image/text generation [31–33], controllable image captioning [34, 35] etc.). For conditional generation tasks, the causal relation of X, Y, T fits in our setting. For relation prediction tasks, we first assume there is an underlying conditional generation process of Y for a given pair of X and T . This is a natural assumption as this is usually how the datasets for this type of task is generated. Then we augment the original dataset using the counterfactual examples generated by our method. In this paper, we try to reduce the spurious correlations contained in both kinds of tasks.

Since we generally cannot observe all possible outcomes Y_1, Y_2, \dots, Y_m for a given X , we derive two different upper bounds of the expected interventional negative log-likelihood $\mathbb{E}_{X, Y_1, Y_2, \dots, Y_m} [-\log p_\theta(Y_1, Y_2, \dots, Y_m | X)]$ using only the observational distribution: one is Implicit CMLE, as it does not involve any explicit generation of counterfactual examples; while the other is Explicit CMLE, as it explicitly generates counterfactual examples during the training process. We test our framework with deep neural networks on two real-world tasks with well-known spurious correlations: natural language inference [24] and image captioning [36]. Compared to regular MLE, we improve the out-of-domain accuracy of NLI on a hard adversarial dataset by 2.9% relatively and beat baselines on human preference evaluations by more than 10%, while maintaining comparable performance

on automated evaluations. Our results show that our learning framework can better capture the underlying causal mechanism and reduce spurious correlations without degrading performance.

2 Related Work

A growing body of work has investigated algorithmic improvements for machine learning model training by leveraging underlying causal mechanisms. One line of work tries to utilize the invariance of causal mechanisms across different environments. Invariant Causal Prediction (ICP) [37] aims to learn a linear invariant causal predictor to identify the causal parents of given target variables with data obtained from different environments. Further refinements on this line of work include nonlinear and nonparametric ICP assessment methods [38] and Invariant Risk Minimization (IRM) where out-of-distribution generalization is enabled by learning a nonlinear invariant causal predictor shared across different environments [12]. However, these methods generally require a set of environments that are both sufficiently diverse to eliminate confounders while maintaining the underlying causal structure. Though this can be achieved by intervening in the non-causal variables in a synthetic or interactive setting, it is very difficult to obtain or even define such environments with complex high-dimensional observational data like text or images. Our proposed CMLE framework only requires a single observational dataset, making it much more practical.

Another line of work approaches this problem with data augmentation. Methods including programmatically editing text to address gender bias [16–18], employing crowd workers to augment training data to capture potential unmeasured variables [39], and manually editing minimal text spans to flip the predicted label [15] have all been proposed to produce counterfactually augmented data (CAD) for improving out-of-domain generalization. Conceptually, in contrast to the first approach that involves interventions on a potentially large number of non-causal variables, CAD directly intervenes on a target variable [40], which is more practical for a specific task. Refinements on this work attempt to better utilize the manually edited or synthetically generated counterfactual data by pairing the factual and counterfactual examples together [41, 42], and leverage local causal structures to generate counterfactual experience in training reinforcement learning algorithms [19]. While human annotators can generate high-quality counterfactual examples that are effective in reducing spurious correlations, they are expensive to obtain and do not easily scale. Meanwhile, our proposed CMLE framework is fully automated, requiring no human annotations.

Our CMLE framework is inspired by a technique for predicting the Individual Treatment Effect (ITE) from observational data [23]. This method only observes one possible outcome of an individual $X = x$ with one binary treatment $T = 0$ or $T = 1$, and it assumes there are no hidden confounders but potentially observed ones. Assuming a similar underlying causal model as ours ($m = 2$) gives an error bound as the sum of the standard generalization error and the distance between the control and treated distributions in a representation space. Improvements on this work include disentangling the observable confounders in ITE using representation learning [43], and estimating the causal effects of linguistic properties [44]. While in this work we do not aim to separate the confounders from the causal factors in X , we try to reduce the spurious correlations caused by the possible confounders contained in X using our proposed CMLE training framework.

3 Method

In this section, we first introduce our problem setting and our goal of Counterfactual Maximum Likelihood Estimation (CMLE). As we cannot observe the counterfactual outcomes in observational data, we propose two different ways of estimating the counterfactual likelihood for deep learning models by deriving two different upper bounds: Implicit CMLE, which is faster in training, and Explicit CMLE, which is more flexible. We also briefly introduce the deep learning architecture we use in our experiments.

3.1 Problem Setting

We consider the scenario with one input variable $X \in \mathcal{X}$ that contain all the confounders, one discrete treatment variable $T \in \{1, 2, \dots, m\}$ where $m \geq 2$, and one outcome variable $Y \in \mathcal{Y}$, as shown in Figure 1a. Note that \mathcal{X} and \mathcal{Y} can be very complicated high dimensional space like text or image and all three variables are observed in the dataset. Suppose the data we observed is

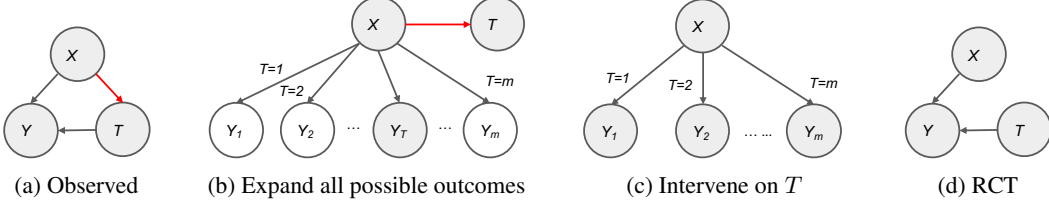


Figure 1: The Structural Causal Model (SCM) assumed by Counterfactual MLE, where (a) and (b) have the same distribution, (c) can be viewed as mimicking the distribution of (d). Shaded nodes means being observed and **red arrows** denote the causal relation causing the spurious correlation.

$\mathcal{D} = \{(x_1, t_1, y_1), (x_2, t_2, y_2), \dots, (x_n, t_n, y_n)\}$ and only x_i 's are sampled i.i.d. In this paper, we adopt the causal notations from [45]. Below we give a formal definition of Structural Causal Model (SCM) [45] that we use to model our framework:

Definition 1. A *Structural Causal Model (SCM)* is a pair $\langle M, p(u) \rangle$, where M is a triple $\langle U, V, F \rangle$ and $p(u)$ is a probability function defined over the domain of U . $U = \{U_1, U_2, \dots, U_n\}$ is a set of background variables (exogenous) that are determined by factors outside the model. $V = \{V_1, V_2, \dots, V_n\}$ is a set of variables (endogenous) and $F = \{f_1, f_2, \dots, f_n\}$ is a set of functions s.t. $V_i = f_i(Pa(V_i), U_i)$, $i = 1, 2, \dots, n$, where $Pa(V_i) \in V \setminus V_i$ are the parents of V_i . We say that " V_j is a direct cause of V_i " if $V_j \in Pa(V_i)$ and illustrate this relation as $V_j \rightarrow V_i$ in a causal graph.

In Figure 1, we omit the exogenous and only show the causal relations between endogenous variables. The shaded nodes indicate that the corresponding variables are observed. Intervention on a specific variable is formalized as fixing the value of this variable to a specific value. This is known as the *do*-operation, changing the causal graph by removing all edges incident to the intervened variable. We denote the outcome of Y corresponding to $do(T = t)$ as Y_t . We expand all the possible outcomes of Y in Figure 1b while we actually can only observe one outcome for each data point in the observational dataset. We also make the following standard assumption:

Assumption 1. (Strong Ignorability Condition) $(Y_1, Y_2, \dots, Y_m) \perp\!\!\!\perp T | X$ and $0 < p(T|X) < 1$.

Under this condition, the counterfactual outcomes are identifiable since $p(Y_t = y|X = x) = p(Y = y|X = x, T = t)$. i.e. The counterfactual likelihood can be written as observable conditional probabilities estimated from data.

Our goal is to eliminate the false causal relation from X to T represented by the red arrow in Figure 1b. To achieve this goal, we define our objective over the interventional distribution $p(X, Y_1, Y_2, \dots, Y_m)$ as shown in Figure 1c, instead of over the observed data distribution $p(X, Y, T)$. Note that there is in fact an environment variable (exogenous) shared among Y_1, Y_2, \dots, Y_m . Here we assume that this variable is also observed and included in X , thus Y_i are mutually independent given X , and we can write $p(Y_1, Y_2, \dots, Y_m|X) = \prod_{i=1}^m p(Y_i|X)$. Here we consider counterfactual maximum likelihood estimation (CMLE) for predicting Y , then the expected error would be:

$$\mathbb{E}_{X, Y_1, Y_2, \dots, Y_m} [-\log p_\theta(Y_1, Y_2, \dots, Y_m|X)] = \mathbb{E}_X \left[\sum_{i=1}^m \mathbb{E}_{Y_i|X} [-\log p_\theta(Y_i|X)] \right] \quad (1)$$

For predicting T , we propose to perform MLE on the distribution shown in Figure 1d, which represents an alternative world that we perform a Randomized Controlled Trial (RCT) with T uniformly distributed on $\{1, 2, \dots, m\}$. This can be estimated by the interventional distribution:

$$\mathbb{E}_{T, X, Y} [-\log p_\theta(T|X, Y)] = \mathbb{E}_{X, Y_1, Y_2, \dots, Y_m} \left[\frac{1}{m} \sum_{i=1}^m -\log p_\theta(T = i|X, Y_T) \right] \quad (2)$$

In the following sections, we first focus on deriving two different upper bounds of the CMLE objective for predicting Y : Implicit CMLE and Explicit CMLE. In Implicit CMLE, we add a regularizer to balance the distribution of X given T in the representation space. For Explicit CMLE, we directly generate counterfactual examples during training. To predict T , we train a classifier using normal MLE on a augmented dataset with *counterfactual examples* generated by $p_\theta(Y_i|X)$ to estimate the joint distribution $p(X, Y_1, Y_2, \dots, Y_m)$. We define a counterfactual example as follows:

Definition 2. A *counterfactual example* is an example (x, t, y) with y sampled from $p(Y_t|X = x)$ s.t. $(x, t, y) \notin \mathcal{D}$ and there is an example $(x, t', y') \in \mathcal{D}$ where $t' \neq t$.

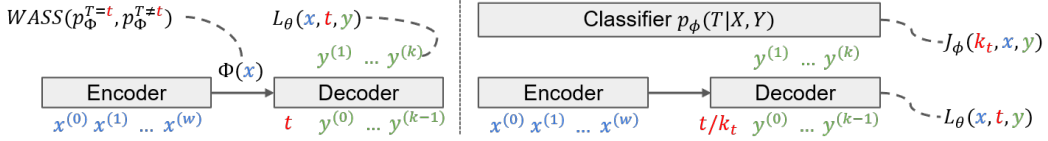


Figure 2: The model architecture of Implicit CMLE (left) and Explicit CMLE (right).

We can rewrite our objective function in Equation 1 as $\mathbb{E}_{X, Y_1, Y_2, \dots, Y_m} [-\log p_\theta(Y_1, Y_2, \dots, Y_m | X)] = \mathbb{E}_x [\sum_{t=1}^m \mathcal{L}_\theta(x, t)]$, by defining the expected loss function of a specific input and treatment as:

Definition 3. We denote the loss function for predicting Y as $L_\theta(x, t, y) = -\log p_\theta(Y_t = y | X = x)$. Then the expected loss function given $X = x$ and $T = t$ is $\mathcal{L}_\theta(x, t) = \mathbb{E}_{Y_t | X=x} [L_\theta(x, t, Y_t)]$.

Because of the Strong Ignorability Assumption, we have $\mathcal{L}_\theta(x, t) > 0$. Then we define an *expected factual loss* $\epsilon_F^{T=t}$ and *expected counterfactual loss* $\epsilon_{CF}^{T=t}$ when observing a specific treatment $T = t$:

Definition 4. The expected factual loss and expected counterfactual loss given $T = t$ are $\epsilon_F^{T=t} = \mathbb{E}_{X|T=t} [\mathcal{L}_\theta(X, t)]$ and $\epsilon_{CF}^{T=t} = \mathbb{E}_{X|T \neq t} [\mathcal{L}_\theta(X, t)]$, respectively.

Here $\epsilon_F^{T=t}$ measures how well the model performs on the observational distribution while $\epsilon_{CF}^{T=t}$ measures how well the model would perform on an alternative world where a different treatment is chosen. Then we can rewrite our CMLE objective as:

$$\mathbb{E}_x [\sum_{t=1}^m \mathcal{L}_\theta(x, t)] = \sum_{t=1}^m [p(T = t) \epsilon_F^{T=t} + p(T \neq t) \epsilon_{CF}^{T=t}] \quad (3)$$

3.2 Implicit CMLE

We consider learning a representation function of X , $\Phi : \mathcal{X} \rightarrow \mathbb{R}^d$, where \mathbb{R}^d is the representation space. Here we make the following assumption about Φ :

Assumption 2. $\Phi : \mathcal{X} \rightarrow \mathbb{R}^d$ is a invertible function. We denote $\Psi : \mathbb{R}^d \rightarrow \mathcal{X}$ as the inverse of Φ . For continuous \mathcal{X} , Ψ also needs to be differentiable to calculate the Jacobian matrix.

Note that this assumption can be fulfilled for neural networks as long as all the activation functions are invertible. We denote the distribution induced by Φ by p_Φ . We can easily transform $p(X|T)$ to $p_\Phi(\Phi(X)|T)$ by a standard change of variable [46, 47]:

Definition 5. For $i \in \{1, 2, \dots, m\}$ and $r \in \mathbb{R}^d$, we denote $p_\Phi^{T=i}(r) := p_\Phi(r|T = i)$. For discrete \mathcal{X} , we simply have $p_\Phi^{T=i}(r) = p(X = \Psi(r)|T = i)$, while for continuous \mathcal{X} , we have $p_\Phi^{T=i}(r) = p(X = \Psi(r)|T = i) \det |\frac{\partial \Psi}{\partial r}|$.

We adopt a similar idea as [23] and use the Integral Probability Metric (IPM) to derive an upper bound of the CMLE objective. IPM is a class of metrics between probability distributions with the following definition [48]:

Definition 6. For two probability density functions p and q defined over \mathcal{S} , we have

$$\text{IPM}_G(p, q) := \sup_{g \in G} \left| \int_{\mathcal{S}} g(s) (p(s) - q(s)) ds \right|$$

Where G is a family of functions $g : \mathcal{S} \rightarrow \mathbb{R}$.

Note that here (and in the rest of our paper) we abuse the notation of integration. If \mathcal{X} is discrete, the integration would become a sum over it. Then we can derive an upper bound for our CMLE objective by Assumption 2, Definition 5 and Equation 3: (See Appendix A.1 for full proof.)

Theorem 1. For a function family G and a constant $B_\Phi > 0$ s.t. $\frac{1}{B_\Phi} \mathcal{L}_\theta(\Psi(r), t) \in G$ for any $r \in \mathbb{R}^d$ and $t \in \{1, 2, \dots, m\}$, the CMLE objective is bounded by:

$$\mathbb{E}_x [\sum_{t=1}^m \mathcal{L}_\theta(x, t)] \leq \sum_{t=1}^m [\epsilon_F^{T=t} + p(T \neq t) B_\Phi \text{IPM}_G(p_\Phi^{T=t}, p_\Phi^{T \neq t})]$$

In this upper bound, we are only left with observational/factual quantities that can be estimated from the observational data. We choose G to be 1-Lipschitz functions, which implies IPM_G to be the Wasserstein distance [49, 50], denoted by $\text{WASS}(\cdot, \cdot)$. Then the empirical CMLE objective using an unbiased estimator of this upper bound can be written as:

$$\arg \min_{\theta} \frac{1}{n} \sum_{i=1}^n \frac{n}{u_{t_i}} L_{\theta}(x_i, t_i, y_i) + \alpha \sum_{j=1}^m \left(1 - \frac{u_j}{n}\right) \text{WASS}(\{\Phi(x_i)\}_{i:t_i=j}, \{\Phi(x_i)\}_{i:t_i \neq j}) \quad (4)$$

Where $u_i = \sum_{j=1}^n \mathbb{1}_{t_j=i}$ and $\mathbb{1}$ is the indicator function. α is a hyperparameter accounting for B_{Φ} and we abuse the notation of $\text{WASS}(\cdot, \cdot)$ to denote an empirical version of Wasserstein distance. The resulting empirical training objective consists of a weighted version of the normal factual loss for empirical risk minimization and a regularization term to draw $p_{\Phi}^{T=i}$ and $p_{\Phi}^{T \neq i}$ closer. $\frac{n}{u_{t_i}}$ accounts for different number of examples with each label and $1 - \frac{u_j}{n}$ account for $p(T \neq j)$ (see Theorem 1). The empirical Wasserstein distance is calculated among examples with different labels in the representation space. In practice, to perform back propagation, we directly compute the gradient of $\text{WASS}(p_{\Phi}^{T=i}, p_{\Phi}^{T \neq i})$ over a single mini-batch, using the algorithm proposed by [51]. (See Appendix B.1 for details.)

3.3 Explicit CMLE

While Implicit CMLE tries to reduce the spurious correlation by learning a better representation of X , we consider directly learning a better approximation of the log likelihood $\log p_{\theta}(Y_t|X)$ by explicitly generating counterfactual examples at training. Here we assume that there is a neural network with parameter ϕ that approximates the true observational distribution $p_{\theta}(T|Y, X)$. We define the following notations:

Definition 7. $p_{\phi}(T|Y, X)$ is an approximate distribution of $p_{\theta}(T|Y, X)$ learned by a neural network parameterized by ϕ using the MLE loss function $J_{\phi}(t, x, y) = -\log p_{\phi}(T = t|Y = y, X = x)$.

Our intuition is that it is directly feasible to learn the normal MLE objective $\mathbb{E}_{X, Y, T}[\log p_{\phi}(T|Y, X)]$ from the observation data, while is infeasible to directly learn the CMLE objective $\mathbb{E}_x[\sum_{t=1}^m \mathcal{L}_{\theta}(x, t)]$. Also, as T is a categorical variable, its distribution is much easier to learn than a potentially complicated Y . We then derive an upper bound of the CMLE objective using Bayes' rule and Jensen's Inequality: (See Appendix A.2 for full proof.)

Theorem 2. By Assumption 1, there exist $0 < \delta_1 < \delta_2 < 1$ s.t. $\delta_1 < p(T|X) < \delta_2$, then we have

$$\mathbb{E}_x \left[\sum_{t=1}^m \mathcal{L}_{\theta}(x, t) \right] \leq \mathbb{E}_{x, t} \left[\frac{1}{\delta_1} \mathbb{E}_{p_{\theta}(Y_t|X=x)} [L_{\theta}(x, t, y)] + \sum_{i \neq t}^m \frac{p(i|x)}{p(t|x)} \mathbb{E}_{p_{\theta}(Y_i|X=x)} [J_{\phi}(i, x, y)] \right] + \mu$$

Where $\mu = (\frac{1}{\delta_1} - \frac{1}{\delta_2} - m + 1) \log m$.

This theorem indicates that we can transfer the counterfactual likelihood of predicting Y into the counterfactual likelihood of T predicted by another conventionally trained model. Since it is expensive to take $m - 1$ samples of y_i from $p_{\theta}(Y_i|X)$ for each training example at train time, we introduce another random variable K_t for each $t \in \{1, 2, \dots, m\}$, such that K_t is uniformly distributed on $\{1, 2, \dots, m\} \setminus \{t\}$. Then the Explicit CMLE objective can be rewritten as:

$$\arg \min_{\theta} \mathbb{E}_{x, t} \left[\mathbb{E}_{p_{\theta}(Y_t|X=x)} [L_{\theta}(x, t, Y_t)] + (m - 1) \delta_1 \mathbb{E}_{K_t} \left[\frac{p(K_t|x)}{p(t|x)} \mathbb{E}_{p_{\theta}(Y_{K_t}|X=x)} [J_{\phi}(K_t, x, Y_{K_t})] \right] \right]$$

Here we ignore the constant term μ in the upper bound and multiply the remaining terms by δ_1 . Note that $\frac{\delta_1}{\delta_2} \leq \frac{p(K_t|x)}{p(t|x)} \leq \frac{\delta_2}{\delta_1}$. In our experiments, we expect $\frac{p(K_t|x)}{p(t|x)}$ to be close to one in the most of the cases, as we would encounter highly biased examples less frequently. However, if the dataset is highly biased with a large variance of $\frac{p(K_t|x)}{p(t|x)}$ across different x , one should consider to first determine this fraction with prior knowledge or with another learning algorithm. In this paper, we regard $\frac{p(K_t|x)}{p(t|x)}$ as

a constant and write the Explicit CMLE objective empirically as:

$$\arg \min_{\theta} \frac{1}{n} \sum_{i=1}^n [L_{\theta}(x_i, t_i, y_i) + \alpha J_{\phi}(k_{t_i}, x_i, y_{\theta}(x_i, k_{t_i}))] \quad (5)$$

Where α is a hyperparameter corresponding to $(m-1)\frac{\delta_1^2}{\delta_2}$, k_{t_i} is randomly sampled from $p(K_{t_i})$ and $y_{\theta}(x_i, k_{t_i})$ is sampled from $p_{\theta}(Y_{k_{t_i}} | X = x)$. Note that since δ_1 and δ_2 are the lower and upper bounds of $p(T|X)$, α is determined by the unknown underlying data distribution. We only sample K_t once and sample the corresponding Y_{K_t} once for computational efficiency. In our implementation, to backpropagate through $p_{\theta}(Y_{k_{t_i}} | X = x)$, we adopt the Gumbel-Softmax approach [52] to deal with the discrete text data, which creates a differentiable sample to replace the non-differentiable discrete variable. For alternative approaches for discrete and continuous \mathcal{Y} , see Appendix B.2.

3.4 CMLE Implementation

While CMLE is a general causal training framework that can be applied to almost any deep learning architecture, in this paper, we primarily consider the Transformer [53] architecture, which excels at modeling sequential data and has been successfully applied to various domains, especially with pretraining on a large amount of data [54, 55]. Here we assume for any $x \in \mathcal{X}$, we can write x as $x = \{x^{(0)}, x^{(1)}, \dots, x^{(w)}\}$ and for any $y \in \mathcal{Y}$, we have $y = \{y^{(0)}, y^{(1)}, \dots, y^{(k)}\}$. We input $T = t$ by prepend a special token/vector corresponding to t as a prefix to the decoder input y . The model architectures of Implicit CMLE and Explicit CMLE are shown in Figure 2.

4 Experiments

We consider two real-world tasks to evaluate the effectiveness of our proposed CMLE causal training framework: Natural Language Inference and Image Captioning. Both tasks have prominent datasets containing well-known spurious correlations; we aim to reduce these correlations’ influence on each target task. In the following sections, we will introduce our experiments in detail and compare the performance of our proposed CMLE against vanilla MLE.

4.1 Natural Language Inference (NLI)

Natural language inference (NLI) [24] is a fundamental task in natural language understanding, which aims to infer the logical relation between a pair of sentences, *premise* and *hypothesis*. Unfortunately, NLI datasets are known to present significant spurious correlations. For example, [3] demonstrated that a machine learning model can non-trivially outperform the majority baseline using only the hypothesis without the premise. One known spurious correlation comes from the background knowledge contained in the premises. i.e. The prediction is based on the background knowledge instead of the logical relation between the premise and the hypothesis. For example, the hypothesis “TV viewing and consumption both begin at about the same time.” would usually be considered to be true from common knowledge. While a fine-tuned RoBERTa [56] also predict this example as entailment, it contradicts its premise “Regular TV viewing typically begins between 2 and 3 years of age, consuming about 10.”. We view the premise sentence as X , the hypothesis sentence as Y , and the label (entailment, neutral, or contradiction) as T . The NLI annotation procedure [24, 57] naturally fits in our causal framework in Figure 1, as the crowd workers are instructed to write a hypothesis that is entailed/neutral/contradicted to a given premise.

We consider three large-scale NLI datasets: SNLI [24], MNLI [25] and ANLI [58]. SNLI and MNLI are considered standard benchmarks. ANLI was constructed as a hard adversarial dataset, with three subsets of increasing difficulty—A1, A2, and A3, to eliminate spurious correlations and balance the data distribution, thus it serves as a great benchmark to evaluate a model’s generalizability. Detailed dataset statistics are shown in Table 1.

For generating counterfactual hypotheses we fine-tune the pre-trained BART large model [59] provided by HuggingFace [60] with 12 encoder and decoder layers. We fine-tune BART on the combined dataset of SNLI and MNLI using both Implicit and Explicit CMLE. We choose $\alpha = 0.003$ for Implicit CMLE and $\alpha = 0.1$ for Explicit CMLE. We predict $p_{\phi}(T|X, Y)$ for Explicit CMLE with a conventionally fine-tuned RoBERTa large model with 24 layers. We call this model NLI-RoBERTa.

Dataset	#train	#dev	#test
A1	16,946	1,000	1,000
A2	45,460	1,000	1,000
A3	100,459	1,200	1,200
ANLI	162,865	3,200	3,200
SNLI	550,152	10,000	10,000
MNLI	392,702	20,000	20,000

Table 1: NLI datasets statistics. ‘ANLI’ refers to ‘A1+A2+A3’.

Method	NLI Accuracy						Generation Consistency	
	A1	A2	A3	ANLI	SNLI	MNLI-m/mm	SNLI (R/H)	MNLI (R/H)
MLE	47.3	26.1	22.4	31.3	92.6	90.6/90.5	N/A	N/A
MLE (w/ Aug)	47.2	25.4	21.7	30.8	92.4	90.4/90.3	65.5/46.8	66.0/48.3
Implicit CMLE	47.0	27.1	24.0	32.2	92.4	90.4/90.5	88.5/69.6	75.1/57.7
Explicit CMLE	47.7	26.8	23.7	32.2	92.4	90.5/90.5	95.2/70.8	85.8/62.4

Table 2: Accuracy of RoBERTa fine-tuned on augmented SNLI + MNLI (left), along with label consistency (accuracy) of the generated hypothesis (right). We report all the results on test sets except on MNLI we use dev sets, where ‘m’ means matched and ‘mm’ means mismatched. ‘R’ indicates evaluations by NLI-RoBERTa and ‘H’ indicates evaluations by human.

We evaluate how consistent our generated hypotheses Y are to their corresponding labels T using both NLI-RoBERTa and human evaluation² in Table 2 (right). In both cases, we perform this assessment by comparing the model- or human-predicted t' against the ground truth t . The accuracy of the NLI-RoBERTa is shown in the first row of Table 2. Both of our CMLE methods significantly outperform the MLE baseline by a large margin on the labeling consistency of the generated hypothesis, which indicates that our CMLE framework can generate Y_t that is truly influenced by $T = t$.

To construct a dataset that mimics sampling from the interventional distribution, we generate two counterfactual examples for each example in the original train dataset of SNLI and MNLI. We filter out the inconsistent examples using NLI-RoBERTa. We generate three augmented datasets using standard MLE, Implicit CMLE, and Explicit CMLE and fine-tune a copy of RoBERTa on each one. The results for these models are presented in rows *MLE (w/ Aug)*, *Implicit CMLE* and *Explicit CMLE* of Table 2 respectively. The baseline *MLE* is NLI-RoBERTa itself. We test the accuracy of all the fine-tuned RoBERTas simultaneously on the regular test sets (MNLI, SNLI) and the out-of-domain adversarial test sets (ANLI). The results in Table 2 show that, while maintaining performance on regular test sets, our proposed CMLE methods significantly outperform both MLE baselines on the adversarial test set. This indicates that CMLE can improve the out-of-domain generalization performance of large deep learning models without hurting the in-domain performance.

4.2 Image Captioning

Image captioning is a fundamental task in studying multimodal interaction. However, image captioning models also suffer severely from spurious correlations [61] that lead to hallucinations. This type of spurious correlation is mainly caused by the typical co-occurrences of objects in images. For example, as toilets are frequently present in bathroom pictures, a captioning model trained by MLE is very likely to hallucinate a ‘toilet’ whenever it sees a ‘bathroom’, even if no toilet is present.

To reduce these hallucination artifacts, we apply our CMLE framework by regarding the image as X , the caption as Y , and whether the caption is hallucinated as T . In our setting, the non-hallucinated captions are ground truth captions written by a human, and the hallucinated captions are generated by image captioning models. The dataset we use is the MSCOCO 2014 dataset [62] which contains 123,287 images of common objects with 5 human-annotated captions per image. We use the Karpathy [63] split with 113,287/5,000/5,000 images in the train/validation/test set respectively. Our implementation is based on [64].

The Transformer architecture we use directly follows [53], with 6 layers in each of the encoder and decoder layers. To construct a dataset with both hallucinated and non-hallucinated captions, we

²All of our human evaluations are conducted via Amazon Mechanical Turk. See Appendix C.3 for details.

Choice (%)	MLE	MLE (w/ Aug)	Implicit CMLE	Explicit CMLE	Tie
Faithfulness	20.7	13.3	28.7	32.0	5.3
Expressiveness	22.7	14.0	27.9	32.7	2.7
Informativeness	21.4	14.7	27.2	32.7	4.0
Preference	17.4	12.6	30.6	32.7	6.7
Accuracy	60.2	54.3	66.9	69.1	N/A

Table 3: Human evaluations of the quality of generated captions. We ask users to choose the best one among four generated captions according to different criterion. *Accuracy* is obtained by asking the user whether a given caption is accurate to the corresponding image or not.

Method	BLEU@4 [65]	METEOR [66]	CIDEr [67]	SPICE [68]	CAHIRs/CHAIRi [61]
MLE	33.1	26.9	106.7	20.0	7.3/5.3
MLE (w/ Aug)	31.3	26.2	102.1	19.6	8.0/5.8
Implicit CMLE	32.0	26.8	105.2	20.0	6.8/4.9
Explicit CMLE	32.1	26.6	105.5	19.9	7.0/5.0

Table 4: Automatic metrics on MSCOCO dataset for image captioning. All the results are reported on the Karpathy test split. Lower CAHIRs and CHAIRi means less object hallucinations.

synthetically generate captions by masking out one object word for each caption and use BERT (large) [54] to fill in an alternative word that aligns with the language model. We estimate the caption hallucination by the CHAIR score [61], which parses the object words in a caption and compares them to the ground truth objects annotated in MSCOCO images and captions. In total, we synthesize 648,550 hallucinated captions for 93,004 images in the training set.

Then we train the transformer model on this augmented dataset of MSCOCO captions with synthetic hallucinated captions using regular MLE and our proposed CMLE methods. We choose $\alpha = 0.0002$ for Implicit CMLE and $\alpha = 0.0001$ for Explicit CMLE. For Explicit CMLE, we fine-tune a pre-trained LXMERT [55] on this augmented dataset as $p_\phi(T|X, Y)$. Here we consider two MLE baselines: The *MLE* baseline is the Transformer model regularly trained on the original MSCOCO dataset, while the *MLE (w/ Aug)* baseline is trained on the augmented dataset.

We conduct user studies on the generated captions as shown in Table 3. In the user study, we let the user choose the best caption among our two baselines and two proposed CMLE methods from the following aspects: *Faithfulness*, *Expressiveness* and *Informativeness*. Faithfulness means how faithful is the generated caption to the corresponding image, which partially measures the extend of hallucinations. Expressiveness means if the generated caption is coherent, grammatically, and semantically correct. Informativeness means if the caption includes most of the information in the image instead of giving a general description. We also let the user choose the caption that best describes the image in their opinion, which is referred to as *Preference* in Table 3. We can see that our proposed CMLE methods outperform the two MLE baselines with a large margin on all the evaluation dimensions which indicates that our methods can not only reduce the hallucination contents in the generated captions but also increase the quality of generated captions in general.

The automatic evaluation results are shown in Table 4, where CHAIRs is the percentage of hallucinated sentences and CHAIRi is the percentage of hallucinated instances (objects). We can see that our CMLE methods outperform both MLE baselines on CHAIR scores, which indicates that our methods can effectively reduce hallucination in image captions. At the same time, the regular scores (BLEU@4, METEOR, CIDEr, SPICE) that measure the similarities between the generated captions and ground truth captions, are comparable between CMLE and the *MLE* baseline. We note that the *MLE (w/ Aug)* baseline on augmented data is significantly worse than the *MLE* baseline on both the automatic scores and human evaluations. We conjecture that this is because the model trained by vanilla MLE is not good at finding the causal relation between the hallucination label T and the caption Y and thus would be confused by the mixture of hallucinated captions and non-hallucinated captions.

4.3 Discussions and Limitations

From both NLI and image captioning experiments, we observe that Explicit MLE is significantly better than Implicit MLE in terms of human evaluations of the generated text, and comparable on other automatic evaluations. We conjecture that this is because that Implicit CMLE only incorporates

counterfactual constraints into the representation of X while Explicit CMLE directly optimizes $p_\theta(Y_t|X)$ when generating the counterfactual examples.

We also note that the improvement on automatic metrics is not that large for both tasks. For NLI, our data augmentation cannot perfectly simulate sampling from the interventional distribution as we only augment two counterfactual examples for each factual example. For Image captioning, as it is difficult to simulate the true distribution of hallucinated captions, the models we trained on the augmented data can be affected by these newly introduced artifacts. On the other hand, the automatic metrics like BLEU only measure the similarity of generated sentences with the observed ground truth which cannot demonstrate the full strength of our methods.

5 Conclusion

Our proposed CMLE framework can be applied to a wide range of learning scenarios with paired inputs and corresponding labels or involving conditional generation. While currently we only consider the spurious correlations caused by the observable confounders under the Strong Ignorability assumption, it is often the case that the confounders are not observed. For example, annotators may have a biased pattern of annotation. As we do not record the information of the annotators, this confounder is considered unobserved. Expanding the current CMLE framework by including the unobserved confounders into the causal model would be an interesting and important future direction.

References

- [1] Jo, J., Y. Bengio. Measuring the tendency of cnns to learn surface statistical regularities, 2017.
- [2] Beery, S., G. Van Horn, P. Perona. Recognition in terra incognita. In *Proceedings of the European Conference on Computer Vision (ECCV)*. 2018.
- [3] Poliak, A., J. Naradowsky, A. Haldar, et al. Hypothesis only baselines in natural language inference. In *Proceedings of the Seventh Joint Conference on Lexical and Computational Semantics*, pages 180–191. Association for Computational Linguistics, New Orleans, Louisiana, 2018.
- [4] Rohrbach, A., L. A. Hendricks, K. Burns, et al. Object hallucination in image captioning. In *Empirical Methods in Natural Language Processing (EMNLP)*. 2018.
- [5] Geirhos, R., P. Rubisch, C. Michaelis, et al. Imagenet-trained cnns are biased towards texture; increasing shape bias improves accuracy and robustness, 2019.
- [6] Zhang, Y., H. Tan, M. Bansal. Diagnosing the environment bias in vision-and-language navigation. In C. Bessiere, ed., *Proceedings of the Twenty-Ninth International Joint Conference on Artificial Intelligence, IJCAI 2020*, pages 890–897. ijcai.org, 2020.
- [7] Kaushik, D., Z. C. Lipton. How much reading does reading comprehension require? a critical investigation of popular benchmarks. In *Proceedings of the 2018 Conference on Empirical Methods in Natural Language Processing*, pages 5010–5015. Association for Computational Linguistics, Brussels, Belgium, 2018.
- [8] Quiñonero-Candela, J., M. Sugiyama, N. D. Lawrence, et al. *Dataset shift in machine learning*. Mit Press, 2009.
- [9] Szegedy, C., W. Zaremba, I. Sutskever, et al. Intriguing properties of neural networks, 2014.
- [10] Ovadia, Y., E. Fertig, J. Ren, et al. Can you trust your model’s uncertainty? evaluating predictive uncertainty under dataset shift. In *NeurIPS*. 2019.
- [11] Filos, A., P. Tigkas, R. Mcallister, et al. Can autonomous vehicles identify, recover from, and adapt to distribution shifts? In H. D. III, A. Singh, eds., *Proceedings of the 37th International Conference on Machine Learning*, vol. 119 of *Proceedings of Machine Learning Research*, pages 3145–3153. PMLR, 2020.
- [12] Arjovsky, M., L. Bottou, I. Gulrajani, et al. Invariant risk minimization, 2020.

- [13] Peters, J., P. Buhlmann, N. Meinshausen. Causal inference using invariant prediction: identification and confidence intervals. *arXiv: Methodology*, 2015.
- [14] Chang, S., Y. Zhang, M. Yu, et al. Invariant rationalization. In *International Conference on Machine Learning*, pages 1448–1458. PMLR, 2020.
- [15] Kaushik, D., E. Hovy, Z. C. Lipton. Learning the difference that makes a difference with counterfactually augmented data. *International Conference on Learning Representations (ICLR)*, 2020.
- [16] Lu, K., P. Mardziel, F. Wu, et al. Gender bias in neural natural language processing. *arXiv preprint arXiv:1807.11714*, 2018.
- [17] Zmigrod, R., S. J. Mielke, H. Wallach, et al. Counterfactual data augmentation for mitigating gender stereotypes in languages with rich morphology. In *Association for Computational Linguistics (ACL)*. 2019.
- [18] Maudslay, R. H., H. Gonen, R. Cotterell, et al. It’s all in the name: Mitigating gender bias with name-based counterfactual data substitution. *arXiv preprint arXiv:1909.00871*, 2019.
- [19] Pitis, S., E. Creager, A. Garg. Counterfactual data augmentation using locally factored dynamics. *Advances in Neural Information Processing Systems*, 33, 2020.
- [20] Pearl, J. Detecting latent heterogeneity. *Sociological Methods & Research*, 46(3):370–389, 2017.
- [21] Greenland, S., J. Pearl, J. M. Robins. Causal diagrams for epidemiologic research. *Epidemiology*, pages 37–48, 1999.
- [22] Shpitser, I., J. Pearl. Identification of conditional interventional distributions. In *Proceedings of the Twenty-Second Conference on Uncertainty in Artificial Intelligence*, UAI’06, page 437–444. AUAI Press, Arlington, Virginia, USA, 2006.
- [23] Shalit, U., F. D. Johansson, D. Sontag. Estimating individual treatment effect: generalization bounds and algorithms. In *International Conference on Machine Learning*, pages 3076–3085. PMLR, 2017.
- [24] Bowman, S. R., G. Angeli, C. Potts, et al. A large annotated corpus for learning natural language inference. *arXiv preprint arXiv:1508.05326*, 2015.
- [25] Williams, A., N. Nangia, S. Bowman. A broad-coverage challenge corpus for sentence understanding through inference. In *Proceedings of the 2018 Conference of the North American Chapter of the Association for Computational Linguistics: Human Language Technologies, Volume 1 (Long Papers)*, pages 1112–1122. Association for Computational Linguistics, 2018.
- [26] Zhang, Y., J. Baldridge, L. He. PAWS: Paraphrase Adversaries from Word Scrambling. In *Proc. of NAACL*. 2019.
- [27] Lan, W., W. Xu. Neural network models for paraphrase identification, semantic textual similarity, natural language inference, and question answering. In *Proceedings of COLING 2018*. 2018.
- [28] Suhr, A., M. Lewis, J. Yeh, et al. A corpus of natural language for visual reasoning. In *Proceedings of the 55th Annual Meeting of the Association for Computational Linguistics (Volume 2: Short Papers)*, pages 217–223. Association for Computational Linguistics, Vancouver, Canada, 2017.
- [29] Gatys, L., A. Ecker, M. Bethge. A neural algorithm of artistic style. *Journal of Vision*, 16(12):326–326, 2016.
- [30] Madaan, A., A. Setlur, T. Parekh, et al. Politeness transfer: A tag and generate approach. In *Proceedings of the 58th Annual Meeting of the Association for Computational Linguistics*, pages 1869–1881. 2020.
- [31] Mirza, M., S. Osindero. Conditional generative adversarial nets. *arXiv preprint arXiv:1411.1784*, 2014.

[32] Hu, Z., Z. Yang, X. Liang, et al. Toward controlled generation of text. In *ICML*, pages 1587–1596. 2017.

[33] Khalifa, M., H. Elsahar, M. Dymetman. A distributional approach to controlled text generation. In *International Conference on Learning Representations*. 2021.

[34] Chen, L., Z. Jiang, J. Xiao, et al. Human-like controllable image captioning with verb-specific semantic roles. *arXiv preprint arXiv:2103.12204*, 2021.

[35] Deng, C., N. Ding, M. Tan, et al. Length-controllable image captioning. *arXiv preprint arXiv:2007.09580*, 2020.

[36] You, Q., H. Jin, Z. Wang, et al. Image captioning with semantic attention. In *Proceedings of the IEEE conference on computer vision and pattern recognition*, pages 4651–4659. 2016.

[37] Peters, J., P. Bühlmann, N. Meinshausen. Causal inference by using invariant prediction: identification and confidence intervals. *Journal of the Royal Statistical Society: Series B (Statistical Methodology)*, 78(5):947–1012, 2016.

[38] Ghassami, A., S. Salehkaleybar, N. Kiyavash, et al. Learning causal structures using regression invariance. In *Advances in Neural Information Processing Systems (NeurIPS)*. 2017.

[39] Srivastava, M., T. Hashimoto, P. Liang. Robustness to spurious correlations via human annotations. *International Conference on Machine Learning (ICML)*, 2020.

[40] Kaushik, D., A. Setlur, E. Hovy, et al. Explaining the efficacy of counterfactually augmented data. *International Conference on Learning Representations (ICLR)*, 2021.

[41] Teney, D., E. Abbasnejad, A. v. d. Hengel. Learning what makes a difference from counterfactual examples and gradient supervision. *arXiv preprint arXiv:2004.09034*, 2020.

[42] Liang, Z., W. Jiang, H. Hu, et al. Learning to contrast the counterfactual samples for robust visual question answering. In *Proceedings of the 2020 Conference on Empirical Methods in Natural Language Processing (EMNLP)*, pages 3285–3292. Association for Computational Linguistics, Online, 2020.

[43] Hassanpour, N., R. Greiner. Learning disentangled representations for counterfactual regression. In *International Conference on Learning Representations*. 2019.

[44] Pryzant, R., D. Card, D. Jurafsky, et al. Causal effects of linguistic properties. *arXiv preprint arXiv:2010.12919*, 2020.

[45] Pearl, J. *Causality*. Cambridge university press, 2009.

[46] Rezende, D., S. Mohamed. Variational inference with normalizing flows. In F. Bach, D. Blei, eds., *Proceedings of the 32nd International Conference on Machine Learning*, vol. 37 of *Proceedings of Machine Learning Research*, pages 1530–1538. PMLR, Lille, France, 2015.

[47] Tran, D., K. Vafa, K. Agrawal, et al. Discrete flows: Invertible generative models of discrete data. *Advances in Neural Information Processing Systems*, 32:14719–14728, 2019.

[48] Müller, A. Integral probability metrics and their generating classes of functions. *Advances in Applied Probability*, pages 429–443, 1997.

[49] Villani, C. *Optimal transport: old and new*, vol. 338. Springer Science & Business Media, 2008.

[50] Sriperumbudur, B. K., K. Fukumizu, A. Gretton, et al. On the empirical estimation of integral probability metrics. *Electronic Journal of Statistics*, 6:1550–1599, 2012.

[51] Cuturi, M., A. Doucet. Fast computation of wasserstein barycenters. In *International conference on machine learning*, pages 685–693. PMLR, 2014.

[52] Jang, E., S. Gu, B. Poole. Categorical reparameterization with gumbel-softmax. *arXiv preprint arXiv:1611.01144*, 2016.

[53] Vaswani, A., N. Shazeer, N. Parmar, et al. Attention is all you need. *arXiv preprint arXiv:1706.03762*, 2017.

[54] Devlin, J., M.-W. Chang, K. Lee, et al. Bert: Pre-training of deep bidirectional transformers for language understanding. *arXiv preprint arXiv:1810.04805*, 2018.

[55] Tan, H., M. Bansal. Lxmert: Learning cross-modality encoder representations from transformers. In *Proceedings of the 2019 Conference on Empirical Methods in Natural Language Processing and the 9th International Joint Conference on Natural Language Processing (EMNLP-IJCNLP)*, pages 5103–5114. 2019.

[56] Liu, Y., M. Ott, N. Goyal, et al. Roberta: A robustly optimized bert pretraining approach. *arXiv preprint arXiv:1907.11692*, 2019.

[57] Williams, A., N. Nangia, S. R. Bowman. A broad-coverage challenge corpus for sentence understanding through inference. *arXiv preprint arXiv:1704.05426*, 2017.

[58] Nie, Y., A. Williams, E. Dinan, et al. Adversarial NLI: A new benchmark for natural language understanding. In *Proceedings of the 58th Annual Meeting of the Association for Computational Linguistics*. Association for Computational Linguistics, 2020.

[59] Lewis, M., Y. Liu, N. Goyal, et al. BART: Denoising sequence-to-sequence pre-training for natural language generation, translation, and comprehension. In *Proceedings of the 58th Annual Meeting of the Association for Computational Linguistics*, pages 7871–7880. Association for Computational Linguistics, Online, 2020.

[60] Wolf, T., L. Debut, V. Sanh, et al. Transformers: State-of-the-art natural language processing. In *Proceedings of the 2020 Conference on Empirical Methods in Natural Language Processing: System Demonstrations*, pages 38–45. Association for Computational Linguistics, Online, 2020.

[61] Rohrbach, A., L. A. Hendricks, K. Burns, et al. Object hallucination in image captioning. In *Proceedings of the 2018 Conference on Empirical Methods in Natural Language Processing*, pages 4035–4045. 2018.

[62] Chen, X., H. Fang, T.-Y. Lin, et al. Microsoft coco captions: Data collection and evaluation server. *arXiv preprint arXiv:1504.00325*, 2015.

[63] Karpathy, A., L. Fei-Fei. Deep visual-semantic alignments for generating image descriptions. In *Proceedings of the IEEE conference on computer vision and pattern recognition*, pages 3128–3137. 2015.

[64] Luo, R., B. Price, S. Cohen, et al. Discriminability objective for training descriptive captions. *arXiv preprint arXiv:1803.04376*, 2018.

[65] Papineni, K., S. Roukos, T. Ward, et al. Bleu: a method for automatic evaluation of machine translation. In *Proceedings of the 40th annual meeting of the Association for Computational Linguistics*, pages 311–318. 2002.

[66] Banerjee, S., A. Lavie. Meteor: An automatic metric for mt evaluation with improved correlation with human judgments. In *Proceedings of the acl workshop on intrinsic and extrinsic evaluation measures for machine translation and/or summarization*, pages 65–72. 2005.

[67] Vedantam, R., C. Lawrence Zitnick, D. Parikh. Cider: Consensus-based image description evaluation. In *Proceedings of the IEEE conference on computer vision and pattern recognition*, pages 4566–4575. 2015.

[68] Anderson, P., B. Fernando, M. Johnson, et al. Spice: Semantic propositional image caption evaluation. In *European conference on computer vision*, pages 382–398. Springer, 2016.

[69] Kingma, D. P., M. Welling. Auto-encoding variational bayes. *arXiv preprint arXiv:1312.6114*, 2013.

[70] Williams, R. J. Simple statistical gradient-following algorithms for connectionist reinforcement learning. *Machine learning*, 8(3-4):229–256, 1992.

A Proofs

In this section, we give full proofs of the two main theorems in the paper.

A.1 Implicit CMLE

Based on Definition 5, the difference between the counterfactual loss and the factual loss can be bounded by the following Lemma:

Lemma A1. *For a function family G and a constant $B_\Phi > 0$ s.t. $\frac{1}{B_\Phi} \mathcal{L}_\theta(\Psi(r), t) \in G$ for any $r \in \mathbb{R}^d$ and $t \in \{1, 2, \dots, m\}$, we have:*

$$\epsilon_{CF}^{T=t} - \epsilon_F^{T=t} \leq B_\Phi \text{IPM}_G(p_\Phi^{T=i}, p_\Phi^{T \neq i})$$

Proof. By Definition 4, we have

$$\epsilon_{CF}^{T=t} - \epsilon_F^{T=t} = \mathbb{E}_{X|T \neq t}[\mathcal{L}_\theta(X, t)] - \mathbb{E}_{X|T=t}[\mathcal{L}_\theta(X, t)]$$

For continuous \mathcal{X} , we have:

$$\begin{aligned} \epsilon_{CF}^{T=t} - \epsilon_F^{T=t} &= \int_{\mathcal{X}} \mathcal{L}_\theta(x, t) (p(X=x|T \neq t) - p(X=x|T=t)) dx \\ &= \int_{\mathbb{R}^d} \mathcal{L}_\theta(\Psi(r), t) (p(X=\Psi(r)|T \neq t) - p(X=\Psi(r)|T=t)) \det \left| \frac{\partial \Psi}{\partial r} \right| dr \end{aligned} \quad (6)$$

$$= \int_{\mathbb{R}^d} \mathcal{L}_\theta(\Psi(r), t) (p_\Phi^{T \neq i}(r) - p_\Phi^{T=i}(r)) dr \quad (7)$$

Where equality 6 is the standard change of variable and equality 7 follows from Definition 5.

For discrete \mathcal{X} we have:

$$\begin{aligned} \epsilon_{CF}^{T=t} - \epsilon_F^{T=t} &= \sum_{\mathcal{X}} \mathcal{L}_\theta(x, t) (p(X=x|T \neq t) - p(X=x|T=t)) \\ &= \int_{\mathbb{R}^d} \mathcal{L}_\theta(\Psi(r), t) (p(X=\Psi(r)|T \neq t) - p(X=\Psi(r)|T=t)) dr \end{aligned} \quad (8)$$

$$= \int_{\mathbb{R}^d} \mathcal{L}_\theta(\Psi(r), t) (p_\Phi^{T \neq i}(r) - p_\Phi^{T=i}(r)) dr \quad (9)$$

Where equality 8 follows from Ψ 's invertibility and equality 9 follows from Definition 5. Then for both continuous and discrete \mathcal{X} we have:

$$\epsilon_{CF}^{T=t} - \epsilon_F^{T=t} = B_\Phi \int_{\mathbb{R}^d} \frac{1}{B_\Phi} \mathcal{L}_\theta(\Psi(r), t) (p_\Phi^{T \neq i}(r) - p_\Phi^{T=i}(r)) dr \quad (10)$$

$$\leq B_\Phi \sup_{g \in G} \left| \int_{\mathbb{R}^d} g(r) (p_\Phi^{T \neq i}(r) - p_\Phi^{T=i}(r)) dr \right| \quad (11)$$

$$= B_\Phi \text{IPM}_G(p_\Phi^{T=t}, p_\Phi^{T \neq t}) \quad (12)$$

Where inequality 10 follows from the definition of supremum and equality 11 follows from $\frac{1}{B_\Phi} \mathcal{L}_\theta(\Psi(r), t) \in G$ and the definition of IPM (Definition 6). \square

Then based on Lemma A1, we can give the following proof for Theorem 1:

Proof.

$$\mathbb{E}_x \left[\sum_{t=1}^m \mathcal{L}_\theta(x, t) \right] = \sum_{t=1}^m [p(T = t) \epsilon_F^{T=t} + p(T \neq t) \epsilon_{CF}^{T=t}] \quad (13)$$

$$= \sum_{t=1}^m [\epsilon_F^{T=t} + p(T \neq t) (\epsilon_{CF}^{T=t} - \epsilon_F^{T=t})] \quad (14)$$

$$\leq \sum_{t=1}^m [\epsilon_F^{T=t} + p(T \neq t) B_\Phi \text{IPM}_G(p_\Phi^{T=t}, p_\Phi^{T \neq t})] \quad (15)$$

Where equality 13 follows from Equation 3, equality 14 follow from $p(T \neq t) = 1 - p(T = t)$ and inequality 15 follows from Lemma A1 we just proved. \square

A.2 Explicit CMLE

Here we give the proof of Theorem 2:

Proof. We first consider expanding the counterfactual part of the CMLE objective in Equation 3 for predicting Y by the Bayes rule and plug in $p_\phi(T|X, Y)$:

$$\begin{aligned} \sum_{t=1}^m p(T \neq t) \epsilon_{CF}^{T=t} &= \sum_{t=1}^m p(T \neq t) \mathbb{E}_{X|T \neq t} [\mathcal{L}_\theta(X, t)] \\ &= \sum_{t=1}^m p(T \neq t) \mathbb{E}_{X|T \neq t} [\mathbb{E}_{Y_t|X=x} [L_\theta(x, t, Y_t)]] \\ &= \sum_{t=1}^m p(T \neq t) \mathbb{E}_{X|T \neq t} [\mathbb{E}_{Y_t|X=x} [-\log p_\theta(Y_t = y|X = x)]] \\ &= \sum_{t=1}^m p(T \neq t) \mathbb{E}_{X|T \neq t} [\mathbb{E}_{Y_t|X} [-\log p_\theta(T = t|Y, X) \\ &\quad - \log p_\theta(T = t|X, Y) + \log p_\phi(T = t|X, Y) \\ &\quad - \log \sum_{i=1}^m p_\theta(Y_i|X) p_\theta(T = i|X) + \log p_\theta(T = t|X)]] \end{aligned}$$

Then we let

$$\begin{aligned} \xi_0 &= \sum_{t=1}^m p(T \neq t) \mathbb{E}_{X|T \neq t} [\mathbb{E}_{Y_t|X} [J_\phi(t, X, Y_t)]] \\ \xi_1 &= - \sum_{t=1}^m p(T \neq t) \mathbb{E}_{X|T \neq t} [\mathbb{E}_{Y_t|X} [\log p_\theta(T = t|X, Y) - \log p_\phi(T = t|X, Y)]] \\ \xi_2 &= \sum_{t=1}^m p(T \neq t) \mathbb{E}_{X|T \neq t} [\mathbb{E}_{Y_t|X} [-\log \sum_{i=1}^m p_\theta(Y_i|X) p_\theta(T = i|X) + \log p_\theta(T = t|X)]] \end{aligned}$$

Where J_ϕ is defined in Definition 7. Then we can rearrange or derive an upper bound for each of these three terms as follow: (note that we abuse the integral as the summation for the discrete case)

$$\begin{aligned}
\xi_0 &= \sum_{t=1}^m p(T \neq t) \mathbb{E}_{X|T \neq t} [\mathbb{E}_{Y_t|X} [J_\phi(t, X, Y_t)]] \\
&= \sum_{t=1}^m p(T \neq t) \int_{\mathcal{X}} p(X = x | T \neq t) [\mathbb{E}_{Y_t|X=x} [J_\phi(t, x, Y_t)]] dx \\
&= \sum_{t=1}^m \int_{\mathcal{X}} p(X = x, T \neq t) [\mathbb{E}_{Y_t|X=x} [J_\phi(t, x, Y_t)]] dx \\
&= \sum_{t=1}^m \int_{\mathcal{X}} \sum_{i \neq t}^m p(T = i | X = x) p(X = x) [\mathbb{E}_{Y_t|X=x} [J_\phi(t, x, Y_t)]] dx \\
&= \sum_{t=1}^m \int_{\mathcal{X}} \sum_{i \neq t}^m \frac{p(T = i | X = x)}{p(T = t | X = x)} p(T = t, X = x) [\mathbb{E}_{Y_t|X=x} [J_\phi(t, x, Y_t)]] dx \\
&= \mathbb{E}_{x,t} \left[\sum_{i \neq t}^m \frac{p(i|x)}{p(t|x)} \mathbb{E}_{Y_t|X=x} [J_\phi(t, x, Y_t)] \right]
\end{aligned}$$

Let $z = \log p_\theta(T = t | X, Y) - \log p_\phi(T = t | X, Y)$, $KL(p||q)$ denotes the KL divergence between two distributions p and q , $H(p)$ denote the entropy of a distribution p . Then we have:

$$\begin{aligned}
\xi_1 &= - \sum_{t=1}^m p(T \neq t) \mathbb{E}_{X|T \neq t} [\mathbb{E}_{Y_t|X} [z]] \\
&= - \sum_{t=1}^m \int_{\mathcal{Y}} \int_{\mathcal{X}} z p_\theta(Y_t = y | X = x) p_\theta(X = x | T \neq t) p_\theta(T \neq t) dx dy \\
&= - \sum_{t=1}^m \int_{\mathcal{Y}} \int_{\mathcal{X}} z p_\theta(T = t | X = x, Y = y) p_\theta(X = x, Y = y) \frac{p_\theta(T \neq t | X = x)}{p_\theta(T = t | X = x)} dx dy \\
&\leq - \left(\frac{1}{\delta_1} - 1 \right) \sum_{t=1}^m \int_{\mathcal{Y}} \int_{\mathcal{X}} \log p_\theta(T = t | X = x, Y = y) p_\theta(T = t | X = x, Y = y) p_\theta(X = x, Y = y) dx dy \\
&\quad + \left(\frac{1}{\delta_2} - 1 \right) \sum_{t=1}^m \int_{\mathcal{Y}} \int_{\mathcal{X}} \log p_\phi(T = t | X = x, Y = y) p_\theta(T = t | X = x, Y = y) p_\theta(X = x, Y = y) dx dy \\
&\quad (16)
\end{aligned}$$

$$\begin{aligned}
&= \mathbb{E}_{X,Y} \left[\sum_{t=1}^m \left[- \left(\frac{1}{\delta_1} - 1 \right) \log p_\theta(T = t | X, Y) + \left(\frac{1}{\delta_2} - 1 \right) \log p_\phi(T = t | X, Y) \right] p_\theta(T = t | X, Y) \right] \\
&= \mathbb{E}_{X,Y} \left[- \left(\frac{1}{\delta_2} - 1 \right) \mathbb{E}_{p_\theta(T|X,Y)} [\log p_\theta(T = t | X, Y) - \log p_\phi(T = t | X, Y)] \right. \\
&\quad \left. + \left(\frac{1}{\delta_1} - \frac{1}{\delta_2} \right) \mathbb{E}_{p_\theta(T|X,Y)} [-\log p_\theta(T = t | X, Y)] \right] \\
&= \mathbb{E}_{X,Y} \left[- \left(\frac{1}{\delta_2} - 1 \right) KL(p_\theta(T | X, Y) || p_\phi(T | X, Y)) + \left(\frac{1}{\delta_1} - \frac{1}{\delta_2} \right) H(p_\theta(T | X, Y)) \right] \\
&\leq \mathbb{E}_{X,Y} \left[0 + \left(\frac{1}{\delta_1} - \frac{1}{\delta_2} \right) \log m \right] = \left(\frac{1}{\delta_1} - \frac{1}{\delta_2} \right) \log m
\end{aligned} \tag{17}$$

Where inequality 16 follows from $\frac{1}{\delta_2} - 1 \leq \frac{p_\theta(T \neq t | X = x)}{p_\theta(T = t | X = x)} \leq \frac{1}{\delta_1} - 1$ and the negativity of log probability. Inequality 17 follows from the positivity of KL divergence and the fact that the largest possible value of entropy of a discrete distribution with m possible value is $\log m$ (can be proven by Jensen's inequality).

By Jensen's inequality, we have:

$$\begin{aligned}
\xi_2 &= \sum_{t=1}^m p(T \neq t) \mathbb{E}_{X|T \neq t} [\mathbb{E}_{Y_t|X} [-\log m \frac{1}{m} \sum_{i=1}^m p_\theta(Y_i|X) p_\theta(T=i|X) + \log p_\theta(T=t|X)]] \\
&\leq \sum_{t=1}^m p(T \neq t) \mathbb{E}_{X|T \neq t} [\mathbb{E}_{Y_t|X} [-\frac{1}{m} \sum_{i=1}^m [\log p_\theta(Y_i|X) + \log p_\theta(T=i|X) + \log m] + \log p_\theta(T=t|X)]] \\
&= \sum_{t=1}^m p(T \neq t) \mathbb{E}_{X|T \neq t} [\mathbb{E}_{Y_t|X} [-\log p_\theta(Y_i|X) - \log m]] \\
&= \sum_{t=1}^m \int_{\mathcal{X}} p(X=x, T \neq t) [\mathbb{E}_{Y_t|X=x} [L_\theta(x, t, Y_t)]] dx - (m-1) \log m \\
&= \sum_{t=1}^m \int_{\mathcal{X}} \frac{p_\theta(T \neq t|X=x)}{p_\theta(T=t|X=x)} p(X=x, T=t) [\mathbb{E}_{Y_t|X=x} [L_\theta(x, t, Y_t)]] dx - (m-1) \log m \\
&\leq (\frac{1}{\delta_1} - 1) \mathbb{E}_{x,t} [\mathbb{E}_{Y_t|X=x} [L_\theta(x, t, Y_t)]] - (m-1) \log m
\end{aligned}$$

Where the last inequality follows from $\frac{p_\theta(T \neq t|X=x)}{p_\theta(T=t|X=x)} \leq \frac{1}{\delta_1} - 1$ and the positivity of $L_\theta(x, t, Y_t)$.

Then by adding ξ_0 , ξ_1 and ξ_2 together, we get:

$$\begin{aligned}
&\sum_{t=1}^m p(T \neq t) \epsilon_{CF}^{T=t} = \xi_0 + \xi_1 + \xi_2 \\
&\leq \mathbb{E}_{x,t} [(\frac{1}{\delta_1} - 1) \mathbb{E}_{Y_t|X=x} [L_\theta(x, t, Y_t)] + \sum_{i \neq t}^m \frac{p(i|x)}{p(t|x)} \mathbb{E}_{Y_t|X=x} [J_\phi(t, x, Y_t)]] \\
&\quad + (\frac{1}{\delta_1} - \frac{1}{\delta_2} - m + 1) \log m
\end{aligned}$$

Then by Definition 4, the whole CMLE objective would be bounded by:

$$\begin{aligned}
\mathbb{E}_x \left[\sum_{t=1}^m \mathcal{L}_\theta(x, t) \right] &= \sum_{t=1}^m [p(T=t) \epsilon_F^{T=t} + p(T \neq t) \epsilon_{CF}^{T=t}] \\
&= \mathbb{E}_{x,t} [\mathbb{E}_{Y_t|X=x} [L_\theta(x, t, Y_t)]] + \sum_{t=1}^m p(T \neq t) \epsilon_{CF}^{T=t} \\
&\leq \mathbb{E}_{x,t} [\frac{1}{\delta_1} \mathbb{E}_{Y_t|X=x} [L_\theta(x, t, Y_t)]] + \sum_{i \neq t}^m \frac{p(i|x)}{p(t|x)} \mathbb{E}_{Y_t|X=x} [J_\phi(t, x, Y_t)] \\
&\quad + (\frac{1}{\delta_1} - \frac{1}{\delta_2} - m + 1) \log m
\end{aligned}$$

□

B Algorithm details

In this section, we give more details of the algorithms we used in the paper.

B.1 Implicit CMLE

We adopt the same algorithm for computing the stochastic gradient of the Wasserstein distance as in [23] as shown in Algorithm 1, where $\text{diag}(v)$ denotes the square matrix with vector v as the diagonal

and $\langle M, N \rangle$ denotes the dot product with two flattened matrices M and N . More specifically, we adopt Algorithm 3 from [51].

Algorithm 1: Computing the stochastic gradient of the Wasserstein distance

Input: A random mini-batch sampled from the observation data and a representation function $\Phi_{\mathbf{w}}$ with current parameter \mathbf{w} . For each $i \in \{1, 2, \dots, m\}$, there are n_i examples $(x_{s_1^{(i)}}, i, y_{s_1^{(i)}}), \dots, (x_{s_{n_i}^{(i)}}, i, y_{s_{n_i}^{(i)}})$ with $t = i$, and $B = \sum_{i=1}^m n_i$. Let $p_i = \frac{u_i}{n}$ as defined in Equation 4;

for $i \in \{1, 2, \dots, m\}$ **do**

Calculate the pairwise L2 distance matrix $M^{(i)}(\Phi_{\mathbf{w}}) \in \mathbb{R}^{n_i \times (B-n_i)}$ between all examples with $t = i$ and $t \neq i$: $M_{kl}^{(i)}(\Phi_{\mathbf{w}}) = \|\Phi_{\mathbf{w}}(x_{s_k^{(i)}}) - \Phi_{\mathbf{w}}(x_{s_l^{(i)}})\|$;

Let $M = M^{(i)}(\Phi_{\mathbf{w}})$, $\lambda = 10/\text{mean}(M)$, $a = (p_i, \dots, p_i) \in \mathbb{R}^{n_i}$ and $b = (1 - p_i, \dots, 1 - p_i) \in \mathbb{R}^{B-n_i}$;

Compute $K = \exp(-\lambda M)$ and $\tilde{K} = \text{diag}(1/a)K$;

Let $u = a$. Then **repeat**

$| u = 1/(\tilde{K}(b/K^T u))$;

until 10 times;

Let $v = b/(K^T u)$ and calculate the approximate optimal transport matrix $T^* = \text{diag}(u)K \text{diag}(v)$;

Calculate the gradient for back propagation: $g_i = \nabla_{\mathbf{w}} \langle T^*, M^{(i)}(\Phi_{\mathbf{w}}) \rangle$;

end

In our implementation, we directly use $\langle T^*, M^{(i)}(\Phi_{\mathbf{w}}) \rangle$ as an approximate of the $\text{WASS}(\cdot, \cdot)$ term in the empirical objective function in Equation 4.

B.2 Explicit CMLE

we separately consider the continuous case and the discrete case of \mathcal{Y} . For continuous $Y \in \mathcal{Y}$, we can use a reparameterization trick as proposed in [69] to separate an auxiliary noise variable Δ from Y as $Y = g_{\theta}(X, T, \Delta)$. Then for each example, we only need to sample the noise Δ and use g_{θ} to get a sample of Y to perform backpropagation on θ .

For the discrete case, we can directly sample a y from $p_{\theta}(Y_t|X = x)$ and then use the REINFORCE algorithm [70] to rewrite the gradient of the second term as $\nabla_{\theta} \mathbb{E}_{p_{\theta}(Y_t|X=x)} [J_{\phi}(i, x, y)] = \mathbb{E}_{p_{\theta}(Y_t|X=x)} [-J_{\phi}(i, x, y) \nabla_{\theta} L_{\theta}(x, t, y)]$. In the paper, we adopt the Gumbel-Softmax approach [52] to deal with the discrete text data, which creates a differentiable sample to replace the non-differentiable discrete variable. More specifically, we substitute a token y sampled from a Multinomial distribution with $p(y = i) = \pi_i$ for $i \in \{1, 2, \dots, V\}$ and $\sum_{i=1}^V \pi_i = 1$ by a continuous vector $z \in \mathbb{R}^V$, with:

$$z_i = \frac{\exp((\log \pi_i + g_i)/\tau)}{\sum_{j=1}^V \exp((\log \pi_j + g_j)/\tau)}$$

Where g_1, g_1, \dots, g_V are sampled i.i.d. from Gumbel(0,1). τ is the Softmax temperature controlling the sharpness of the sample z across the V categories. For a more detailed discussion of all three methods mentioned above, see [52].

C Experiment Details

Our code is written with PyTorch. We use the same data split as the original dataset or as stated in Section 4 and we choose our hyperparameters by the validation performance on the dev sets.

C.1 Natural Language Inference

Datasets: The SNLI dataset is licensed under a Creative Commons Attribution-ShareAlike 4.0 International License. The majority of the MNLI corpus is released under the OANC's license, and

the whole MNLI dataset is in the public domain in the United States. ANLI is licensed under Creative Commons-Non Commercial 4.0.

Training details: We train all the models using the Trainer module provided by Huggingface [60] with Adam optimizer. For fine-tuning the BART-based generation models, we use a learning rate of 5e-5 and a total batch size of 128 and train for 3 epochs. Note that in our train dataset, T is pretty balanced, so we treat all $\frac{n}{u_i} = 3$ and we merge this constant into the learning rate of the Implicit CMLE method (see Equation 4). For fine-tuning the RoBERTa based classification models, we adopt the same setting as [58], that is we use a learning rate of 1e-5 and a total batch size of 128 and train for 2 epochs. We conduct all our experiments on NVIDIA Titan RTX GPUs (24GB), except fine-tuning BART using the Explicit CMLE method, which is trained on NVIDIA Tesla V100 GPUs (16GB). For each experiment, we parallelize our data across four GPUs. For fine-tuning BART, MLE and Implicit CMLE takes about 13 hours to train on Titan RTX GPUs, while Explicit CMLE takes about 8 hours to train on Tesla V100 GPUs (would take a much longer time on Titan RTX GPUs). For fine-tuning RoBERTa, the augmentation methods take about 12 hours to train while the un-augmented MLE takes about 4 hours to train on NVIDIA Titan RTX GPUs.

C.2 Image Captioning

Dataset: MSCOCO 2014 dataset is licensed under a Creative Commons Attribution 4.0 License.

Training details: We train all the models using the image captioning codebase provided by [64] with Adam optimizer. Since we train all the models from scratch, for CMLE methods, we first train the Transformer model with the normal MLE objective for the first 3 epochs and then switch to the CMLE objective to stabilize the training. For all methods, we use a learning rate of 1e-4 and a total batch size of 100 and train for 25 epochs. Note that we force the balance of T among each batch, so we treat all $\frac{n}{u_i} = 2$ and we merge this constant into the learning rate of the Implicit CMLE method (see Equation 4). We conduct all our experiments on NVIDIA Titan RTX GPUs (24GB). For augmented methods, MLE and Implicit CMLE take about 40 hours to train on a single GPU while the Explicit CMLE takes about 80 hours to train on two GPUs. The un-augmented MLE takes about 20 hours to train on a single GPU.

C.3 Mechanical Turk Details

We conduct all of our human evaluations and user studies via Amazon Mechanical Turk. Our studies only include simple multiple-choice problems that do not involve collecting any personal information. We also first manually check the examples to make sure there are no offensive contents. We are happy to provide our IRB approval document upon request.

C.3.1 Assessing Generated NLI Hypothesis Quality

We choose 200 premises with corresponding generated hypothesis from each of the three methods, *MLE (w/ Aug)*, *Implicit CMLE* and *Explicit CMLE*, such that each hypothesis is different from each other. We produce Human Intelligence Tasks (HITs) as follows:

At the top of the HIT page, the crowdworker is shown the following instructions:

You are given a premise sentence and a hypothesis sentence below. Your job is to determine that whether the hypothesis is entailed, neutral or contradicted to the premise sentence. Here is the explanation of what are entailed, neutral and contradicted:

- Entailed: the hypothesis is definitely correct about the premise.
- Neutral: the hypothesis might be correct about the premise.
- Contradicted: the hypothesis is definitely incorrect about the premise.

Along with the following example and explanations:

Premise: Two dogs are running through a field.

Hypothesis 1: There are animals outdoors. [Entailed. Because dogs are animals and the field must be outdoors.]

Hypothesis 2: Some puppies are running to catch a stick. [Neutral. Because dogs are not necessarily

Survey Instructions (Click to expand)

You are given a premise sentence and a hypothesis sentence below. Your job is to determine that whether the hypothesis is entailed, neutral or contradicted to the premise sentence. Here is the explanation of what are entailed, neutral and contradicted:

- Entailed: the hypothesis is definitely correct about the premise.
- Neutral: the hypothesis might be correct about the premise.
- Contradicted: the hypothesis is definitely incorrect about the premise.

Example:

Premise : Two dogs are running through a field.

- **Hypothesis 1** : There are animals outdoors. [Entailed. Because dogs are animal and field must be outdoors.]
- **Hypothesis 2** : Some puppies are running to catch a stick. [Neutral. Because dogs are not necessarily puppies and running doesn't mean they are catching a stick. However, there is a possibility that the hypothesis is a more detailed description of the same event, but we can't know that from the premise alone.]
- **Hypothesis 3** : The pets are sitting on a couch. [Contradicted. Because 'pets' refers to the 'dogs'. If the dogs are running then they can't be sitting on a couch. The premise and the hypothesis can't both be true.]

Premise: This church choir sings to the masses as they sing joyous songs from the book at a church.

- **Hypothesis 1**: A choir is singing at a wedding. [Entailed ▾]
- **Hypothesis 2**: A church choir sings to the masses as they sing joyous songs from the book at a wedding. [Entailed ▾]
- **Hypothesis 3**: The church choir is singing hymns. [Entailed ▾]

Premise: There is a plane in the sky.

- **Hypothesis**: There is a white plane in the sky. [Entailed ▾]

Figure 3: Natural language inference human evaluation interface.

puppies and running doesn't mean they are catching a stick. However, there is a possibility that the hypothesis is a more detailed description of the same event, but we can't know that from the premise alone.]

Hypothesis 3: *The pets are sitting on a couch. [Contradicted. Because 'pets' refers to the 'dogs'. If the dogs are running then they can't be sitting on a couch. The premise and the hypothesis can't both be true.]*

After the instructions, the crowd worker is shown one premise with three different hypotheses and is asked to determine whether each hypothesis is entailed, neutral and contradicted to the given premise. After this question, a simple sanity checking question is also shown to check whether the worker correctly understands the instructions:

Premise: There is a plane in the sky.

Entailed Hypothesis: There is an airplane.

Neutral Hypothesis: There is a white plane in the sky.

Contradicted Hypothesis: There is no plane in the sky.

In each HIT, the same premise is shown with one of the three hypotheses at random. We only collect the example with this sanity check question answered correctly. Figure 3 is a screenshot of the user interface.

We paid 0.3 US dollar for each question and we paid \$119 in total for this human evaluation. We estimate the time of answering each question would be approximately 90-120 seconds as the questions involve understanding the logical relationships between the sentences and there is a very detailed instruction to read. So the hourly wage for crowd workers would be \$9 to \$12.

C.3.2 Assessing Generated Image Caption Quality

We choose 150 images with corresponding generated captions from each of the four methods, *MLE*, *MLE (w/ Aug)*, *Implicit CMLE* and *Explicit CMLE*, such that each caption is different from each other. We produce Human Intelligence Tasks (HITs) for as follows:

At the top of the HIT page, the crowd worker is shown the source image, with the instructions “*Look at the image, then read the following 4 descriptions. For each, answer if it is an accurate description (is it a fair description of the image?) Then, answer 4 comparison questions, choosing which sentence is the most correct, has the best style, describes the most information, and is the best overall.*”

In the **descriptions** section of the HIT page, the crowd worker then sees the four candidate description sentences (in random order) in the left-hand column. Next to each sentence, in a right-hand column,

Instructions

Look at the image, and then read the following 4 **descriptions**. For each, answer if it is an **accurate** description (is it a fair description the image?) Then, answer 4 **comparison questions**, choosing which sentence is the most correct, has the best style, describes the most information, and is best overall.

Image



Description 1

a dog that is laying down in a pool .

Is this description accurate?

Yes No

Description 2

a brown dog standing outside of a pool .

Is this description accurate?

Yes No

Description 3

a large brown dog laying across a pool .

Is this description accurate?

Yes No

Description 4

a dog is sitting in the corner of a swimming pool .

Is this description accurate?

Yes No

Comparison Questions

Which description is the most correct (does not describe anything that is *not* present in the image)?

Description 1 Description 2 Description 3 Description 4 None of them

Which sentence has the most correct grammar and best style?

Description 1 Description 2 Description 3 Description 4 None of them

Which description accurately describes the most information in the image?

Description 1 Description 2 Description 3 Description 4 None of them

Overall, which caption would you choose to best describe the image?

Description 1 Description 2 Description 3 Description 4 None of them

Submit

Figure 4: Image captioning user study interface.

is the question “*Is this description accurate?*” and a radio button with which the crowd worker can answer “*yes*” or “*no*”.

They are then shown a set of four **comparison questions** to rank the captions in terms of *correctness*, *expressiveness*, *informativeness*, and general *preference*. The questions are:

Correctness: *Which description is the most correct (does not describe anything that is *not* present in the image)?*

Expressiveness: *Which sentence has the most correct grammar and best style?*

Correctness: *Which description accurately describes the most information in the image?*

Correctness: *Overall, which caption would you choose to best describe the image?*

For each comparison question, the crowdworkers choose between five multiple-choice answers: *Description 1*, *Description 2*, *Description 3*, *Description 4*, or *None of them*.

Each HIT is shown to a total of 7 crowd workers. To produce a human assessment of the **accuracy** of a given caption generation technique, we simply count the rate at which all respondents answer “*yes*” to the “*Is this description accurate?*” questions for each model’s generated examples. To assess the **faithfulness**, **expressiveness**, **informativeness**, and **preference**, we choose the “*best*” generated caption for each comparison using the majority vote of the 7 crowd workers. If the majority choose “*none of them*” or there is a tie, we assign that image as a tie. We then produce each model’s

comparison question scores by counting the rates at which their captions were rated “best” for each question. Figure 4 is a screenshot of the user interface.

We paid 0.1 US dollar for each question and we paid \$126 in total for this user study. We estimate the time of answering each question would be approximately 30-40 seconds as the questions do not involve heavy reading or reasoning. So the hourly wage for crowd workers would be \$9 to \$12.

D Broader Impact

Techniques for provably reducing the influence of spurious correlations on classification decisions and generative system outputs could be a boon for the reliability of and trust in general public-facing AI systems. Considering that these spurious correlations driven by observable confounders are present across a wide array of datasets and tasks, the techniques we propose herein could be broadly applicable for general system reliability improvements in supervised learning settings.

As for risks, we estimate that our proposed methods are not particularly rife for abuse, and pose a low level of danger broadly comparable to other innovations in optimizers, loss functions, and neural network architectures. We believe there is not a significant risk of any code or data produced for this study being used to nefarious ends. A possible risk to the environment is induced by the use of large pre-trained models, which would consume a large amount of computing resources at training. This issue can be mitigated by adopting more efficient training algorithms and compress the number of trainable parameters with a small trade-off in performance.